Title
Topologically Protected Quantum State Transfer via Edge States in Superconducting Circuits

Author
Tian, Lin

Publication Date
2019-01-08

Peer reviewed

Topologically Protected Quantum State Transfer via Edge States in Superconducting Circuits

Feng Mei,[1,2] Gang Chen,[1,2,*] Lin Tian,[3,†] Shi-Liang Zhu,[4,5,6,‡] and Suotang Jia[1,2]

[1] *State Key Laboratory of Quantum Optics and Quantum Optics Devices, Institute of Laser Spectroscopy, Shanxi University, Taiyuan, Shanxi 030006, China*
[2] *Collaborative Innovation Center of Extreme Optics, Shanxi University, Taiyuan, Shanxi 030006, China*
[3] *School of Natural Sciences, University of California, Merced, California 95343, USA*
[4] *National Laboratory of Solid State Microstructures, School of Physics, Nanjing University, Nanjing 210093, China*
[5] *Guangdong Provincial Key Laboratory of Quantum Engineering and Quantum Materials, SPTE, South China Normal University, Guangzhou 510006, China*
[6] *Synergetic Innovation Center of Quantum Information and Quantum Physics, University of Science and Technology of China, Hefei 230026, China*

(Dated: February 15, 2018)

Robust quantum state transfer (QST) is an indispensable ingredient in scalable quantum information processing. Here we present an experimentally feasible scheme for robust QST via topologically protected edge states in superconducting circuits. Using superconducting X-mon qubits with tunable couplings, the generalized Su-Schrieffer-Heeger models with topological magnon bands can be constructed. A novel entanglement-dependent topological Thouless pumping can be directly observed in this system. More importantly, we show that single-qubit states and entanglement can be robustly transferred with high fidelity in the presence of qubit-coupling imperfection, which is a hallmark of topological protection. This approach is experimentally applicable to a variety of quantum systems.

To realize large-scale quantum information processing, quantum states need to be coherently transferred between distant nodes in a quantum network [1–3]. Several techniques have been proposed to implement robust QST in various physical systems, such as photon pulse shaping of atoms coupled optical cavity [4, 5], transfer via spin chains and spin-wave engineering [6–10], frequency conversion via optomechanical interface [11], and quantum error correction [12, 13]. However, the inevitable existence of environmental noise and parameter imperfection can strongly limit the fidelity of QST.

Topological phenomena, rooted in the global property of topological matters, provide a natural protection against perturbation and disorder [14, 15]. Non-abelian anyons generated in topological materials assisted with braiding operations have been intensively explored for topological quantum computing [16, 17]. The topologically protected Hall conductance is insensitive to disorder in the electronic systems [18, 19]. Moreover, topologically protected edge states can be used for robust electronic and photonic transport [20, 21]. Recently, topological properties have been employed for QST via chiral spin liquids, which relies on the realization of controllable coupling between qubits and the spin liquids and is challenging to implement [22]. Therefore, it would be highly desirable to have a topologically protected QST that can be implemented in practical qubit systems.

Here we present an experimentally feasible mechanism for the robust QST via the topological edge states in superconducting circuits [23]. By connecting superconducting X-mon qubits into a one-dimensional chain with tunable couplings [24, 25], the generalized Su-Schrieffer-Heeger (SSH) type of qubit chains [26, 27] can be constructed, which support topological magnon bands featured by topological winding numbers or Chern numbers. We find that entanglement-related dynamical topological phenomena can be used to directly measure the topological invariants of the magnon bands. In contrast to recent experiments on topological properties in superconducting circuits [28–33], which focus on the parameter space of the qubits and resonators, our study aims at the intrinsic topological properties of the magnon bands. More importantly, we show that an adiabatic QST of single-qubit states and entanglement can be realized via topological edge states. Using a numerical simulation, we demonstrate that the QST is topologically protected by the finite energy gap between the bulk and the edge states and the transfer fidelities have a plateau at the value of unity in the presence of qubit-coupling imperfection, which is a hallmark of topologically protected processes. This protocol only requires tunable coupling between the qubits and can be implemented in various qubit systems, such as trapped ions [34–36], cold atoms [37, 38], nitrogen vacancy centers [39], electronic spins [40] and optomechanical systems [41]. Our result can hence lead to future studies of scalable quantum networks with topologically protected quantum channels.

Generalized SSH-type qubit chains and topological magnon bands.– The generic setup for robust QST of single- or two-qubit states is illustrated in Fig. 1(a). This protocol is applicable to various qubit systems with tunable coupling, but for concreteness, here we focus on

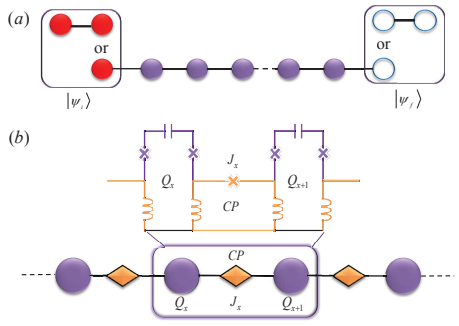

FIG. 1. (a) The transfer of unknown single-qubit or entangled states from the qubits inside the left box to the qubits inside the right box through the intermediate qubit chain. Each circle represents a qubit. (b) The implementation of the qubit chain with superconducting X-mon qubits. The qubits Q_x and Q_{x+1} are inductively coupled by the tunable coupler CP with coupling strength J_x.

superconducting qubit chain. Adjacent qubits are coupled inductively via a tunable Josephson junction coupler shown in Fig. 1(b). The coupling strength J_x can be tuned smoothly by varying the current in the coupler. This setup has been realized in recent experiments on superconducting X-mon qubits [24, 25]. The corresponding Hamiltonian is $\hat{H} = \sum_x J_x \hat{\sigma}_x^+ \hat{\sigma}_{x+1}^- + \text{H.c.}$ with $\hat{\sigma}_x^+ = |e\rangle_x\langle g|$ for the qubit at site x. Assume that the frequencies of all qubits are the same and omit the qubit frequencies from the Hamiltonian. Let $J_x = g_0 + g_1 \cos\varphi_x$, where $g_{0,1}$ are the coupling constants and $\varphi_x = 2\pi x/p + \theta$ with p being the number of qubits in one unit cell and θ being a control parameter. In the Supplemental Materials [42], we show that the qubit operators can be converted to magnon operators with the MatsubaraMatsuda transformation, where the qubit excitations generate magnon bands [42]. Here we only consider qubit states with a single excitation. Because the number of excitations is conserved in our system, the Hilbert space under consideration can be restricted to the space spanned by single-excitation states $\{\hat{\sigma}_x^+|G\rangle\}$, where $|G\rangle = |gg\cdots g\rangle$ is the magnon vacuum and $|g\rangle$ is the ground state of each qubit.

For $p = 2$, each unit cell contains two qubits labeled by a_x and b_x, respectively. The Hamiltonian becomes

$$\hat{H} = \sum_{x=1}^{N} (J_1 \hat{\sigma}_{a_x}^+ \hat{\sigma}_{b_x}^- + J_2 \hat{\sigma}_{b_x}^+ \hat{\sigma}_{a_{x+1}}^- + \text{H.c.}) \tag{1}$$

with $J_m = g_0 + (-1)^m g_1 \cos\theta$ $(m = 1, 2)$ and N being the number of unit cells. This qubit chain resembles the SSH model in the single-magnon space [42]. It has two magnon bands and their topological features are characterized by the winding number $\nu = [1 + \text{sgn}(g_0 g_1 \cos\theta)]/2$ [42]. For positive $g_0 g_1$, the magnon band is in a nontrivial (trivial) topological phase with $\nu = 1$ $(\nu = 0)$ when $\theta \in (-\pi/2, \pi/2)$ $[\theta \in (\pi/2, 3\pi/2)]$.

The winding number is a basic topological invariant to characterize the topological bands. Here we show that it can be directly measured from quantum dynamics. Define the center of excitation difference between the a- and b-type qubits as $\hat{P}_d = \sum_{x=1}^{N} x(\hat{P}_{a_x}^e - \hat{P}_{b_x}^e)$ with $\hat{P}_q^e = |e\rangle_q\langle e|$ $(q = a_x, b_x)$. Its dynamics can be revealed from $\bar{P}_d(t) = \langle\psi(0)|e^{i\hat{H}t}\hat{P}_d e^{-i\hat{H}t}|\psi(0)\rangle$ with $|\psi(0)\rangle$ being the initial state. Let the qubits in the central unit be initially prepared in the Bell state $|\chi\rangle = (|ge\rangle + |eg\rangle)/\sqrt{2}$ and all other qubits in their ground states [42], i.e., $|\psi(0)\rangle = |gg\cdots\chi\cdots gg\rangle$. We find that $\bar{P}_d(t)$ is related to the winding number as [42]

$$\nu = \lim_{T\to\infty} \frac{2}{T} \int_0^T dt\, \bar{P}_d(t) \tag{2}$$

with T being the total evolution time. Equation (2) provides a new method to detect the winding number through measuring the dynamical evolution of the qubit excitation, which may also open a prospect in exploring topology-dependent quantum dynamics.

For the case of $p > 2$, the generalized SSH-type qubit chain has p magnon bands. Different from $p = 2$ case, their topological features are characterized by Chern numbers. Here we illustrate $p = 3$ as an example. In such case, each unit cell has three qubits labeled as a, b, and c, respectively, and the Hamiltonian reads

$$\hat{H} = \sum_{x=1}^{N} (J_1 \hat{\sigma}_{a_x}^+ \hat{\sigma}_{b_x}^- + J_2 \hat{\sigma}_{b_x}^+ \hat{\sigma}_{c_x}^- + J_3 \hat{\sigma}_{c_x}^+ \hat{\sigma}_{a_{x+1}}^- + \text{H.c.}) \tag{3}$$

with $J_m = g_0 + g_1 \cos(2\pi m/3 + \theta)$ $(m = 1, 2, 3)$. The Hamiltonian (3) supports three topological magnon bands. Suppose the Chern number for the n-th magnon band is C_n $(n = 1, 2, 3)$. It is found that there are two different topological magnon phases characterized by the Chern numbers $\{C_1 = -1, C_2 = 2, C_3 = -1\}$ and $\{C_1 = 2, C_2 = -4, C_3 = 2\}$, respectively [42]. The topological transition between these two phases can be tuned by changing the ratio g_0/g_1 [42]. So various topological phase transitions can be observed in this simple system

The Chern numbers can be detected by an entanglement-dependent Thouless pumping with θ adiabatically tuned. For illustration, we take $g_0 = g_1$, under which the three magnon bands have the Chern numbers $\{C_1 = -1, C_2 = 2, C_3 = -1\}$. Let $\theta(t) = \Omega t + \varphi_0$ with Ω being the ramping frequency and φ_0 being the initial phase. The total pumping time is then $T_p = 2\pi/\Omega$. At time $t = 0$, let $\theta(0) = \varphi_0 = \pi$. The coupling strengths are then $J_{1,2} = 3g_1/2$ and $J_3 = 0$, i.e., the unit cells are isolated with zero inter-cell coupling. The eigenstates of a single magnon excitation in an isolated unit cell are the entangled states $|\chi_{1,3}\rangle = (|egg\rangle \mp \sqrt{2}|geg\rangle + |gge\rangle)/2$ and $|\chi_2\rangle = (|egg\rangle - |gge\rangle)/\sqrt{2}$. Let the initial state be $|\psi_n(0)\rangle = |ggg\cdots\chi_n\cdots ggg\rangle$, with one unit cell in the entangled state $|\chi_n\rangle$ and all other qubits in their ground states [42]. As θ is swept from $t = 0$ to $t = T_p$, the state

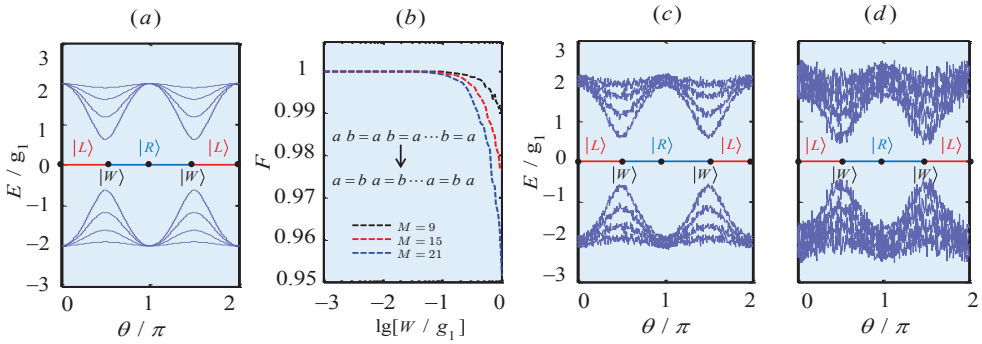

FIG. 2. The energy spectra of the $p = 2$ SSH model vs θ for the imperfection strength (a) $W = 0$, (c) $W = 0.6g_1$ and (d) $W = 0.8g_1$. The total qubit number is 9. (b) The fidelity of the QST vs the imperfection strength. The total qubit number is 9 (black), 15 (red), and 21 (blue) with $\Omega = \{0.04g_1, 0.02g_1, 0.01g_1\}$. The other parameter is $g_0 = g_1$.

in the initial unit cell experiences an adiabatic pumping and the entanglement will propagate to other unit cells. Define the center of excitation as $\hat{P}_s = \sum_{x=1}^{N} x(\hat{P}^e_{a_x} + \hat{P}^e_{b_x} + \hat{P}^e_{c_x})$. The time-dependence of the center of excitation is described by $\bar{P}_{sn}(t) = \langle\psi_n(t)|\hat{P}_s|\psi_n(t)\rangle$ for an initial entanglement $|\chi_n\rangle$ $(n = 1, 2, 3)$. Our analytical derivation [42] shows that the change of the average center of excitation after one pumping circle is equal to the band-dependent Chern number with

$$C_n = \bar{P}_{sn}(T_p) - \bar{P}_{sn}(0). \tag{4}$$

This dynamical process yields an entanglement-dependent topological pumping [42], which introduces quantum entanglement into the original Thouless particle pumping [43–47] and has not been reported before. Based on this pumping scheme, we can measure the Chern numbers in a practical superconducting circuit with a few qubits [42].

Robust single-qubit quantum state transfer.– The bulk states of the $p = 2$ SSH model are characterized by the winding number. The bulk-edge correspondence, which relates topological invariants to the topologically protected excitations localized at the boundaries, guarantees the existence of the topologically protected edge states in this system [14, 15]. In the following, we will show that the edge state in a chain of odd number $(2N - 1)$ qubits can be exploited as a topologically protected quantum channel to realize the robust QST. The wave function of this edge state has the form

$$|\psi_E(\theta)\rangle = \sum_{x=1}^{N}(-1)^x \left(\frac{g_0 - g_1\cos\theta}{g_0 + g_1\cos\theta}\right)^x \hat{\sigma}^+_{a_x}|G\rangle, \tag{5}$$

which only occupies the a-type qubits [42]. Let $g_0 = g_1$, the edge state concentrates towards the left (right) end when $\theta \in (-\pi/2, \pi/2)$ $[\theta \in (\pi/2, 3\pi/2)]$. In particular, at $\theta = 0$ (π), the coupling strength becomes $J_1 = 0$ $(J_2 = 0)$ with the leftmost (rightmost) qubit decoupled from the rest of the qubit chain, and the edge state is $|L\rangle = |egg\cdots gg\rangle$ $(|R\rangle = |gg\cdots ge\rangle)$. At $\theta = \pi/2$ or $3\pi/2$, the edge state is a W-state $|W\rangle = \sum_{x=1}^{N}(-1)^x\hat{\sigma}^+_{a_x}|g\rangle^{\otimes N}/\sqrt{N}$ with equal excitation in all the a-type qubits.

An unknown single-qubit state can be transferred adiabatically via the edge mode. Let $\theta(t) = \Omega t$, where θ is swept from 0 at $t = 0$ to π at the final time. At time $t = 0$, the leftmost qubit is prepared in the unknown state $\alpha|e\rangle + \beta|g\rangle$ and all other qubits are in their ground states. The state of the qubit chain is then $|\psi_i\rangle = \alpha|L\rangle + \beta|G\rangle$, which is in a superposition of the edge state at $\theta = 0$ and the ground state $|G\rangle$ with no excitation. During the sweeping, the state evolves from $|L\rangle \to |W\rangle \to |R\rangle$, as θ is varied from $0 \to \pi/2 \to \pi$ (see Fig. 2(a)). The final state of the qubit chain is $|\psi_f\rangle = \alpha|R\rangle + \beta|G\rangle$ with the rightmost qubit in the state $\alpha|e\rangle + \beta|g\rangle$. To ensure high fidelity of QST, it is required that the process be adiabatic in the entire process, i.e., $\sqrt{g_1\Omega}$ needs to be smaller than the energy gap between the bulk and the edge states. For example, we can choose $\Omega = 0.01g_1$ for a chain of 21 qubits, which has an energy gap larger than $0.1g_1$. For superconducting X-mon qubits with $g_1/2\pi = 250$ MHz, the time of QST is $t_f = \pi/\Omega = 0.2\,\mu$s, much shorter than typical qubit decoherence times [24, 25].

In practical, the system parameters cannot be perfectly tuned to exact values due to the intrinsic fluctuations in device fabrication. In our scheme, the main imperfection factor is the qubit-coupling imperfection that far exceeds the effect of qubit decoherence [48, 49]. This imperfection can be described by the Hamiltonian

$$\hat{H}_d = \sum_x \delta J_x \hat{\sigma}^+_x \hat{\sigma}^-_{x+1} + \text{H.c.}, \tag{6}$$

where $\delta J_x = W\delta$ with W being the imperfection strength and $\delta \in [-0.5, 0.5]$ being a random number. For each δJ_x, we choose 100 samples to perform the numerical simulation throughout this work. The fidelity is obtained by averaging over the results of all samples. In Fig. 2(b), we numerically calculate the fidelity $F = |\langle R|\psi(t_f)\rangle|$ as a function of the imperfection strength. A wide plateau

at $F \approx 1$ appears for $W \lesssim 0.1g_1$, where the energy gap remains large enough to protect QST. The appearance of the plateau is a hallmark of the topologically protected QST, which ensures high transfer fidelity, and the plateau can also be observed in the two-qubit entanglement transfer studied below. With current technology, the imperfection strength is $\sim 5-10\%$ of the coupling constant g_1. Our simulation shows that the fidelity can exceed 0.998 for $W = 0.1g_1$ when the qubit chain size is over 20. This indicates that nearly perfect QST can be realized in practical circuits with our protocol.

This topological protection is endowed by the chiral symmetry that is intrinsic to the SSH model. Such symmetry requires a symmetric energy spectrum with each positive eigenenergy E accompanied by a negative eigenenergy $-E$, implying existence of zero energy edge mode. In the presence of qubit-coupling imperfection, the system Hamiltonian still obeys the chiral symmetry, i.e., $\hat{\Gamma}(\hat{H}+\hat{H}_d)\hat{\Gamma}^{-1} = -(\hat{H}+\hat{H}_d)$, where $\hat{\Gamma} = \prod_x(\hat{\sigma}^+_{a_x}\hat{\sigma}_{a_x} - \hat{\sigma}^+_{b_x}\hat{\sigma}_{b_x})$ is the chiral operator [26, 27]. As a result, the zero-energy edge state is insensitive to imperfection in the couplings. This is verified by our numerical calculation of the energy spectrum of the qubit chain in the presence of qubit-coupling imperfection, as given in Fig. 2(c, d).

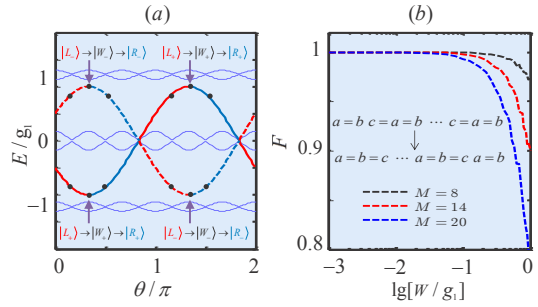

FIG. 3. (a) The energy spectra of the $p = 3$ generalized SSH model vs θ with a chain of 8 qubits and $g_0 = 0$. (b) The fidelities of entanglement transfer vs the imperfection strength. The total qubit number is 8 (black), 14 (red), and 20 (blue) with $\Omega = \{0.01g_1, 0.004g_1, 0.001g_1\}$, respectively.

Robust entanglement transfer.– For the $p = 3$ generalized SSH model with $3N-1$ qubits, there exists one pair of edge states (see Fig. 3(a)). Here one edge state exists within each bulk energy gap. The energies and the wave functions of the edge states can be solved analytically as $E_\pm = \pm[g_0 + g_1\cos(2\pi/3+\theta)]$ and

$$|\psi_\pm\rangle = \sum_x \left[\mp\frac{g_0+g_1\cos(4\pi/3+\theta)}{g_0+g_1\cos\theta}\right]^x \frac{\hat{\sigma}^+_{a_x} \pm \hat{\sigma}^+_{b_x}}{\sqrt{2}}|G\rangle, \tag{7}$$

which only occupies the a- and b-type qubits [42]. Let $g_0 = 0$. The edge states concentrate near the left end when $\theta \in (-\pi/6, \pi/3)\cup(5\pi/6, 4\pi/3)$, and occupy the right end when $\theta \in (\pi/3, 5\pi/6)\cup(4\pi/3, 11\pi/6)$.

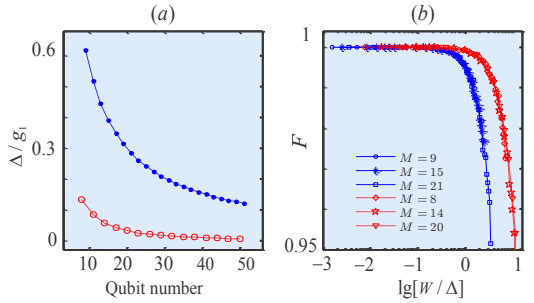

FIG. 4. (a) The bulk-edge energy gap vs qubit number for the $p = 2$ (blue) and $p = 3$ (red) SSH models. (b) The fidelities of the QST vs $\lg[W/\Delta]$. Blue: the $p = 2$ SSH model with 9 (circle), 15 (star), and 21 (square) qubits; red: the $p = 3$ generalized SSH model with 8 (diamond), 14 (pentagram), and 20 (triangle) qubits. Other parameters are the same as those in Fig. 2 and Fig. 3.

Specifically, at $\theta = \pi/6, 7\pi/6$ $(\pi/2, 3\pi/2)$, the coupling strength $J_1 = 0$ $(J_2 = 0)$, and the two leftmost (rightmost) qubits are decoupled from the rest of the qubit chain. The edge states are $|L_\pm\rangle = |\chi_\pm\rangle|ggg\cdots ggg\rangle$ $(|R_\pm\rangle = |ggg\cdots ggg\rangle|\chi_\pm\rangle$, where $|\chi_\pm\rangle = (|eg\rangle \pm |ge\rangle)/\sqrt{2}$ are Bell states. At $\theta = \pi/3, 4\pi/3$, the edge states are W states $|W_\pm\rangle = \sum_x(-1)^x(\hat{\sigma}^+_{a_x} + \hat{\sigma}^+_{b_x})|g\rangle^{\otimes(2N)}/\sqrt{2N}$.

At time $t = 0$, let $\theta(0) = \pi/6$ with the system prepared in the edge states $|L_\pm\rangle$. θ is then swept linearly as $\theta(t) = \theta(0) + \Omega t$. After a ramping time $t_p = \pi/3\Omega$, $\theta = \pi/2$. During the ramping, the state evolves adiabatically as $|L_\pm\rangle \to |W_\pm\rangle \to |R_\pm\rangle$ and reaches the final state $|R_\pm\rangle$, which is localized in the right end. The entangled state $|\chi_\pm\rangle$ is thus transferred from the left end to the right end. With $g_1/2\pi = 250$ MHz, we choose $\Omega = 0.001g_1$ for a chain of 20 qubits, which gives $t_f = 0.67\,\mu$s and satisfies the adiabatic condition. We also numerically simulate the transfer process in the presence of finite qubit-coupling imperfection and obtain the transfer fidelity $F = |\langle R_+|\psi(t_f)\rangle|$ for the state $|\chi_+\rangle$. As shown in Fig. 3(b), the fidelity exhibits a plateau at $F \approx 1$, demonstrating the topological protection of the entanglement transfer. A fidelity above 0.99 can be achieved for an imperfection strength $W \lesssim 0.07g_1$.

Discussions.– For the QST protocols to succeed, the adiabatic condition needs to be obeyed. Denote the energy gap as Δ, which is the smallest energy separation between the bulk and the edge states in the related parameter range. The adiabatic theorem requires that $|dH/dt| < \Delta^2$. For the SSH models, this corresponds to $\sqrt{g_1\Omega} < \Delta$. For a chain of 50 qubits, $\Delta \sim g_1/10$. Hence a ramping rate $\Omega < 0.01g_1$ is required. Because the energy gap decreases with the size of the qubit chain, as shown in Fig. 4(a), more stringent requirement on the ramping rate or other approaches, such as the shortcuts to adiabaticity [52, 53], will be needed to maintain the transfer fidelity in a longer qubit chain.

Furthermore, we study the transfer fidelity of single-qubit and entanglement as a function of the imperfection $\lg[W/\Delta]$. In Fig. 4(b), the transfer fidelities for qubit chains with different size are plotted, which fall near a single curve for a given transfer regardless of the size of the chain size. Both curves have a wide plateau with high fidelity exceeding 0.99 when $W < 0.1\Delta$. Our result verifies that QST via the edge states is topologically protected and insensitive to small perturbations in the Hamiltonian.

Our system can be implemented with current technology of superconducting quantum devices. A chain of 9 X-mon qubits has been realized in experiments and the implementation of longer chains is promising in near future [50, 51]. With a typical coupling strength of $g_1/2\pi = 250$ MHz, the ramping time for QST can be achieved in sub-micron seconds, much shorter than the decoherence times for the X-mon qubits [48, 49].

Acknowledgment.– This work is supported by the National Key R&D Program of China under Grants No. 2017YFA0304203 and No. 2016YFA0301803; the NSFC under Grants No. 11674200, No. 11604392, No. 11434007 and No. 91636218; the PCSIRT under Grant No. IRT13076; SFSSSP; OYTPSP; SSCC; and 1331KSC. L.T. is supported by the National Science Foundation (USA) under Award Numbers DMR-0956064 and PHY-1720501, the UC Multicampus-National Lab Collaborative Research and Training under Award No. LFR-17-477237, and the UC Merced Faculty Research Grants 2017.

* chengang971@163.com
† ltian@ucmerced.edu
‡ slzhu@nju.edu.cn

[1] M. A. Nielsen, and I. L. Chuang, Quantum computation and quantum information (Cambridge University Press, 2000).
[2] H. J. Kimble, The quantum internet, *Nature* **453**, 1023 (2008).
[3] T. E. Northup, and R. Blatt, Quantum information transfer using photons, *Nature Photon.* **8** 356 (2014)
[4] J. I. Cirac, P. Zoller, H. J. Kimble, and H. Mabuchi, Quantum state transfer and entanglement distribution among distant nodes in a quantum network, *Phys. Rev. Lett.* **78**, 3221 (1997).
[5] D. N. Matsukevich, and A. Kuzmich, Quantum state transfer between matter and light, *Science* **306**, 663 (2004).
[6] S. Bose, Quantum communication through an unmodulated spin chain, *Phys. Rev. Lett.* **91**, 207901 (2003).
[7] M. Christandl, N. Datta, A. Ekert, and A. J. Landahl, Perfect state transfer in quantum spin networks, *Phys. Rev. Lett.* **92**, 187902 (2004).
[8] S. Bose, Quantum communication through spin chain dynamics: an introductory overview, *Contemp. Phys.* **48**, 13 (2007).
[9] Z. Song and C. P. Sun, Quantum information storage and state transfer based on spin systems, *Low Temp. Phys.* **31**, 686 (2005).
[10] N. Y. Yao, L. Jiang, A. V. Gorshkov, Z. X. Gong, A. Zhai, L. M. Duan, and M. D. Lukin, Robust quantum state transfer in random unpolarized spin chains, *Phys. Rev. Lett.* **106**, 040505 (2011).
[11] L. Tian, Optoelectromechanical transducer: reversible conversion between microwave and optical photons, *Ann. Phys. (Berlin)* **527**, 1 (2015).
[12] B. Vermersch, P. O. Guimond, H. Pichler, and P. Zoller, Quantum state transfer via noisy photonic and phononic waveguides, *Phys. Rev. Lett.* **118**, 133601 (2017).
[13] Z. L. Xiang, M. Z. Zhang, L. Jiang, and P. Rabl, Intracity quantum communication via thermal microwave networks, *Phys. Rev. X* **7**, 011035 (2017).
[14] M. Z. Hasan and C. L. Kane, Topological insulators, *Rev. Mod. Phys.* **82**, 3045 (2010).
[15] X. L. Qi and S. C. Zhang, Topological insulators and superconductors, *Rev. Mod. Phys.* **83**, 1057 (2011).
[16] C. Nayak, S. H. Simon, A. Stern, M. Freedman, and S. D. Sarma, Non-Abelian anyons and topological quantum computation, *Rev. Mod. Phys.* **80**, 1083 (2008).
[17] N. Cooper, Non-Abelian anyons and topological quantum computation, *Adv. Phys.* **57**, 539 (2008).
[18] K. v. Klitzing, G. Dorda, and M. Pepper, New method for high-accuracy determination of the fine-structure constant based on quantized Hall resistance, *Phys. Rev. Lett.* **45**, 494 (1980).
[19] D. J. Thouless, M. Kohmoto, M. P. Nightingale, and M. den Nijs, Quantized Hall conductance in a two-dimensional periodic potential, *Phys. Rev. Lett.* **49**, 405 (1982).
[20] K. S. Novoselov, Z. Jiang, Y. Zhang, S. V. Morozov, H. L. Stormer, U. Zeitler, J. C. Maan, G. S. Boebinger, P. Kim, and A. K. Geim, Room-temperature quantum Hall effect in graphene, *Science* **315**, 1379 (2007).
[21] L. Lu, J. D. Joannopoulos, and M. Soljacic, Topological photonics, *Nature Photon.* **8**, 821 (2014).
[22] N. Y. Yao, C. R. Laumann, A. V. Gorshkov, H. Weimer, L. Jiang, J. I. Cirac, P. Zoller, and M. D. Lukin, Topologically protected quantum state transfer in a chiral spin liquid, *Nature Commun.* **4**, 1585 (2013).
[23] M. H. Devoret, and R. J. Schoelkopf, Superconducting circuits for quantum information: an outlook, *Science* **339**, 1169 (2013).
[24] R. Barends, J. Kelly, A. Megrant, D. Sank, E. Jeffrey, Y. Chen, Y. Yin, B. Chiaro, J. Mutus, C. Neill, P. O'Malley, P. Roushan, J. Wenner, T. C. White, A. N. Cleland, and J. M. Martinis, Coherent Josephson qubit suitable for scalable quantum integrated circuits, *Phys. Rev. Lett.* **111**, 080502 (2013).
[25] Y. Chen, C. Neill, P. Roushan, N. Leung, M. Fang, R. Barends, J. Kelly, B. Campbell, Z. Chen, B. Chiaro, A. Dunsworth, E. Jeffrey, A. Megrant, J. Y. Mutus, P. J. J. O'Malley, C. M. Quintana, D. Sank, A. Vainsencher, J. Wenner, T. C. White, Michael R. Geller, A. N. Cleland, and J. M. Martinis, Qubit architecture with high coherence and fast tunable coupling, *Phys. Rev. Lett.* **113**, 220502 (2014).
[26] W. P. Su, J. R. Schrieffer, and A. J. Heeger, Solitons in Polyacetylene, *Phys. Rev. Lett.* **42**, 1698 (1979).
[27] J. K. Asbóth, L. Oroszlány, and A. Pályi, A short course on topological insulators: band structure and edge states

in one and two dimensions, *Lecture Notes in Physics* (2016).

[28] M. D. Schroer, M. H. Kolodrubetz, W. F. Kindel, M. Sandberg, J. Gao, M. R. Vissers, D. P. Pappas, A. Polkovnikov, and K. W. Lehnert, Measuring a topological transition in an artificial spin-1/2 system, *Phys. Rev. Lett.* **113**, 050402 (2014).

[29] P. Roushan, C. Neill, Y Chen, M. Kolodrubetz, C. Quintana, N. Leung, M. Fang, R. Barends, B. Campbell, Z. Chen, B. Chiaro, A. Dunsworth, E. Jeffrey, J. Kelly, A. Megrant, J. Mutus, P. J. J. O'Malley, D. Sank, A. Vainsencher, J. Wenner, T. White, A. Polkovnikov, A. N. Cleland, and J. M. Martinis, Observation of topological transitions in interacting quantum circuits, *Nature* **515**, 241 (2014).

[30] P. Roushan, C. Neill, A. Megrant, Y. Chen, R. Babbush, R. Barends, B. Campbell, Z. Chen, B. Chiaro, A. Dunsworth, A. Fowler, E. Jeffrey, J. Kelly, E. Lucero, J. Mutus, P. J. J. O'Malley, M. Neeley, C. Quintana, D. Sank, A. Vainsencher, J. Wenner, T. White, E. Kapit, H. Neven, and J. Martinis, Chiral ground-state currents of interacting photons in a synthetic magnetic field, *Nature Phys.* **13**, 146 (2017).

[31] V. V. Ramasesh, E. Flurin, M. Rudner, SI. iddiqi, and N. Y. Yao, Direct probe of topological invariants using bloch oscillating quantum walks, *Phys. Rev. Lett.* **118**, 130501 (2017).

[32] E. Flurin, V. V. Ramasesh, S. Hacohen-Gourgy, L. S. Martin, N. Y. Yao, and I. Siddiqi, Observing topological invariants using quantum walks in superconducting circuits. *Phys. Rev. X* **7**, 031023 (2017).

[33] O. Viyuela, A. Rivas, S. Gasparinetti, A. Wallraff, S. Filipp, and M.A. Martin-Delgado, Observation of topological Uhlmann phases with superconducting qubits. arXiv: 1607.08778v2.

[34] R. Blatt, and D. Wineland, Entangled states of trapped atomic ions, *Nature* **453**, 1008 (2008).

[35] J. Brox, P. Kiefer, M. Bujak, T. Schaetz, and T. Landa, Spectroscopy and Directed Transport of Topological Solitons in Crystals of Trapped Ions, *Phys. Rev. Lett.* **119**, 153602 (2017).

[36] J. Zhang, G. Pagano, P. W. Hess, A. Kyprianidis, P. Becker, H. Kaplan, A. V. Gorshkov, Z. X. Gong, and C. Monroe, Observation of a many-body dynamical phase transition with a 53-qubit quantum simulator, arXiv: 1708.01044 (2017).

[37] T. Fukuhara, A. Kantian, M. Endres, M. Cheneau, P. Schauß S. Hild, D. Bellem, U. Schollwöck, T. Giamarchi, C. Gross, I. Bloch, and S. Kuhr, Quantum dynamics of a mobile spin impurity, *Nature Phys.* **9**, 235 (2013).

[38] H. Bernien, S. Schwartz, A. Keesling, H. Levine, A. Omran, H. Pichler, S. Choi, A. S. Zibrov, M. Endres, M. Greiner, V. Vuletić, and M. D. Lukin, Probing many-body dynamics on a 51-atom quantum simulator, arXiv: 1707.04344 (2017).

[39] M. W. Doherty, N. B. Manson, P. Delaney, F. Jelezko, J. Wrachtrup, and L. C. L. Hollenberg, The nitrogen-vacancy colour centre in diamond, *Phy. Rep.* **528**, 1 (2013).

[40] D. D. Awschalom, L. C. Bassett, A. S. Dzurak, E. L. Hu, and J. R. Petta, Quantum spintronics: engineering and manipulating atom-like spins in semiconductors, *Science* **339**, 1174 (2013).

[41] M. Metcalfe, Applications of cavity optomechanics, *Appl. Phys. Rev.* **1**, 031105 (2014).

[42] See the Supplementray Materials.

[43] D. J. Thouless, Quantization of particle transport, *Phys. Rev. B* **27**, 6083 (1983).

[44] S. Nakajima, T. Tomita, S. Taie, T. Ichinose, H. Ozawa, L. Wang, M. Troyer, and Y. Takahashi, Topological Thouless pumping of ultracold fermions, *Nature Phys.* **12**, 296 (2016).

[45] M. Lohse, C. Schweizer, O. Zilberberg, M. Aidelsburger, and I. Bloch, A Thouless quantum pump with ultracold bosonic atoms in an optical superlattice, *Nature Phys.* **12**, 350 (2016).

[46] F. Mei, J. B. You, D. W. Zhang, X. C. Yang, R. Fazio, S. L. Zhu, and L. C. Kwek, Topological insulator and particle pumping in a one-dimensional shaken optical lattice, *Phys. Rev. A* **90**, 063638 (2014).

[47] H. I. Lu, M. Schemmer, L. M. Aycock, D. Genkina, S. Sugawa, and I. B. Spielman, Geometrical pumping with a Bose-Einstein condensate, *Phys. Rev. Lett.* **116**, 200402 (2016).

[48] H. Paik, D. I. Schuster, L. S. Bishop, G. Kirchmair, G. Catelani, A. P. Sears, B. R. Johnson, M. J. Reagor, L. Frunzio, L. I. Glazman, S. M. Girvin, M. H. Devoret, and R. J. Schoelkopf, Observation of high coherence in Josephson junction qubits measured in a three-dimensional circuit QED architecture, *Phys. Rev. Lett.* **107**, 240501 (2011).

[49] M. Reagor, H. Paika, G. Catelanib, L. Y. Sun, C. Axline, E. Holland, I. M. Pop, N. A. Maslukc, T. Brecht, L. Frunzio, M. H. Devoret, L. Glazman, and R. J. Schoelkopfd, Reaching 10 ms single photon lifetimes for superconducting aluminum cavities, *Appl. Phys. Lett.* **102**, 192604 (2013).

[50] J. Preskill, Quantum computing and the entanglement frontier, arXiv.org: 1203.5813 (2012).

[51] S. Boixo, S. V. Isakov, V. N. Smelyanskiy, R. Babbush, N. Ding, Z. Jiang, M. J. Bremner, J. M. Martinis, and H. Neven, Characterizing quantum supremacy in near-term devices, arXiv: 1608.00263 (2016).

[52] M. V. Berry, Transitionless quantum driving, *J. Phys. A* **42**, 365303 (2009).

[53] Y. X. Du, Z. T. Liang, Y. C. Li, X. X. Yue, Q. X. Lv, W. Huang, X. Chen, H. Yan, and S. L. Zhu, Experimental realization of stimulated Raman shortcut-to-adiabatic passage with cold atoms, *Nature Commun.* **7**, 12479 (2016).